

RESEARCH ARTICLE

10.1029/2018JA025810

Key Points:

- Positive correlation has been observed between solar 10.7-cm flux and zonal drift velocity of EPBs over Indian low-latitude region
- Intense enhancement in OI 630.0-nm emission is occurred during disturbed night causing reduction in zonal drift velocity of EPBs
- Latitudinal variation in zonal drift velocity of EPBs on disturbed night affected the morphology of EPBs

Correspondence to:

A. K. Sharma,  
aks\_phy@unishivaji.ac.in

Citation:

Gurav, O. B., Sharma, A. K., Ghodpage, R. N., Nade, D. P., Chavan, G. A., Gaikwad, H. P., & Patil, P. T. (2018). Zonal drift velocity of equatorial plasma bubbles during ascending phase of 24th solar cycle using all-sky imager over Kolhapur, India. *Journal of Geophysical Research: Space Physics*, 123, 10,266–10,282. <https://doi.org/10.1029/2018JA025810>




Received 22 JUN 2018

Accepted 24 OCT 2018

Accepted article online 11 NOV 2018

Published online 10 DEC 2018

## Zonal Drift Velocity of Equatorial Plasma Bubbles During Ascending Phase of 24th Solar Cycle Using All-Sky Imager Over Kolhapur, India

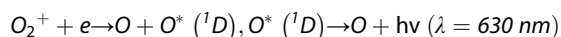
O. B. Gurav<sup>1</sup>, A. K. Sharma<sup>1,2</sup> , R. N. Ghodpage<sup>3</sup>, D. P. Nade<sup>4</sup> , G. A. Chavan<sup>5</sup> , H. P. Gaikwad<sup>1</sup>, and P. T. Patil<sup>3</sup>

<sup>1</sup>Space and Earth Science Laboratory, Department of Physics, Shivaji University, Kolhapur, India, <sup>2</sup>Now at School of Physics, Shri Mata Vaishno Devi University, Katra Kakryal, Katra, J&K, India, <sup>3</sup>Medium Frequency Radar, Indian Institute of Geomagnetism, Shivaji University Campus, Kolhapur, India, <sup>4</sup>Department of Physics, Sanjay Ghodawat University, Kolhapur, India, <sup>5</sup>Department of Physics, Ahmednagar College, Ahmednagar, India

**Abstract** This paper reports the statistical analysis of zonal drift velocity of equatorial plasma bubbles (EPBs) inferred from advanced optical technique (all-sky imager) with OI 630.0-nm airglow emission from January to April of 2011 to 2013. Over 143 nights of observations have been carried out using all-sky imager over low-latitude station Kolhapur (16.8°N, 74.2°E; 10.6°N dip latitude), out of which 58 nights showed signatures of EPBs. We study the hourly, monthly, and seasonal variation in zonal drift velocity of EPBs. Also, the magnetically disturbed nights ( $A_p > 18$ ) are separately studied. It is observed that (a) the daily peak zonal drift velocity is seen to be positively correlated to corresponding daily averaged 10.7-cm solar flux. (b) The zonal drift velocity is found to be larger in the equinox months than that of winter months. (c) During the disturbed nights the zonal drift velocity gets slower and one of the disturbed nights showed the latitudinal variation in zonal drift velocity during the development phase of EPBs before midnight hours. We suggest that this variation might be occurred due to the disturbance dynamo electric fields at low latitude, which reduces the EPBs' eastward velocity. (d) The zonal drift velocity of EPBs presented in this paper is in good agreement with the previous studies as well as the HWM-07 model values.

### 1. Introduction

The depletions in the  $F$  region ionospheric densities, nowadays termed as equatorial plasma bubbles (EPBs), are the manifestation as the dark bands in optical data recorded by all-sky imager (ASI), which provides a unique opportunity to study the spatial and temporal variation of these structures. The EPBs are considered as harmful for communication and navigation systems as it causes the error in the signal which come across these structures. This communication includes the high frequency and very high frequency, VHF (megahertz and gigahertz), which are widely used for ground based as well as satellite communication. The EPBs are the turbulent structures of depleted plasma often consisting of smaller-scale size structures at their sharp edges, which are responsible for the scintillations in the radio waves. The night airglow emission coming from the ionospheric heights is very much important as it provides the information about the electrodynamics of the ionosphere in terms of electron density. The OI 630.0-nm nightglow emission is produced at the bottomside of the ionospheric  $F$  region, at about 250- to 300-km altitude, by the dissociative recombination process as follows:



and this is commonly used to investigate the thermospheric-ionospheric processes at  $F$  region altitudes (Pimenta, Fagundes, et al., 2003).

The OI 630.0-nm emission is a good indicator of electrodynamical processes occurring in the ionosphere, and it is widely used for irregularity monitoring and investigations. The ASI (Figure 1a) is capable to monitor large-scale structures called EPBs over a very large geographical area ( $\sim 12 \times 10^5 \text{ km}^2$  at an altitude of 250 km) from Kolhapur. It is quite efficient as it provides a wide spatial coverage ( $\sim 1,220 \text{ km}$  in diameter,  $140^\circ$  field of view [FOV], Figure 1b) and captures 2-D footage of the evolution and morphology of large-scale irregularities in real time. None of other technique has this capability to retrieve the real-time 2-D

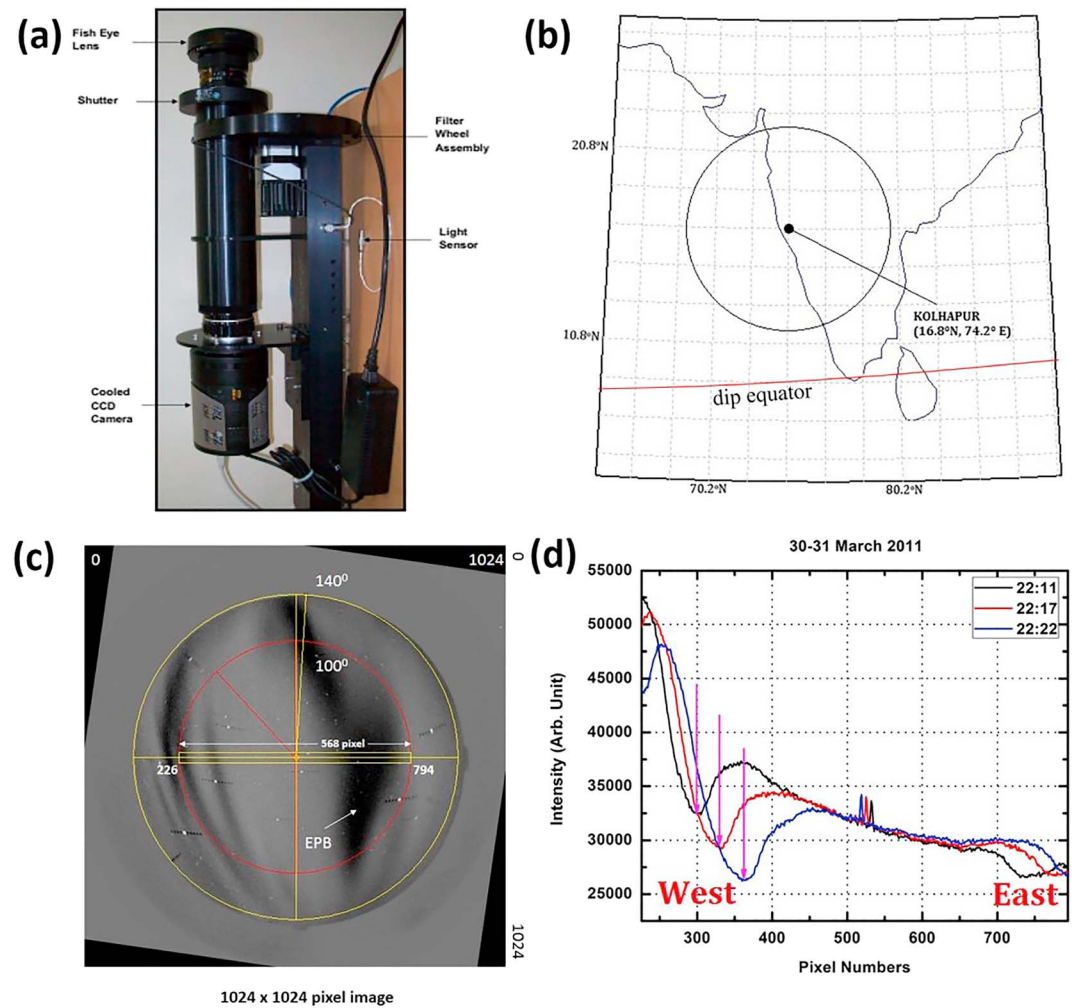


**Figure 1.** (a) The photograph of all-sky imager (ASI) setup installed at Kolhapur. (b) The field of view of ASI as 140°, which covers horizontal distance of 1,220 km. (c) The ASI sample image in pixel coordinates with 140° field of view (FOV; yellow circle) and 100° FOV (red circle). The horizontal 20 pixel strip around zenith within 100° FOV is taken for intensity extraction. (d) The extracted intensity plots with 20-pixel strip around zenith ( $\pm 10$  pixels) for successive three images on 30–31 March 2011. The downward pink arrows show the traversal of equatorial plasma bubbles from west to east.

images of ionospheric irregularities. It is pretty handy and can easily transport from one location to another. The equatorial spread  $F$  (ESF) associated with ionospheric irregularities are considered to be generated in the bottomside  $F$  layer at the geomagnetic equator during postsunset period, and the regions of depleted plasma density grow upward nonlinearly (Mukherjee, 2003). These plasma depletions move vertically, diffuse along the magnetic field lines, and reach to the lower latitudes. The peak height of airglow emitting regions where the footprints of these depleted flux tubes encounter corresponds to a severe decrease in the intensity, which is a function of the plasma density in the ionosphere.

The different aspects of EPBs have been studied by many researchers such as occurrence characteristics (e.g., Candido et al., 2011; Makela et al., 2004; Sahai et al., 1994; Sharma, Gurav, et al., 2017; Sharma et al., 2014; Sun et al., 2016), morphology and evolution (e.g., Aggson et al., 1996; Huba et al., 2015; Narayanan et al., 2016; Wu et al., 2017), statistical features of EPBs (e.g., Narayanan et al., 2017; Sinha & Raizada, 2000; Sun et al., 2016), and zonal drift velocity (e.g., Abalde et al., 2004; Immel et al., 2004; Mukherjee & Shetti, 2008; Nade et al., 2013; Paulino et al., 2011; Pimenta et al., 2001; Taori et al., 2013; Yao & Makela, 2007). However, there are different techniques to monitor and study the evolution and characteristics of these large-scale structures (EPBs) such as incoherent scatter radar (e.g., Fejer et al., 1991), VHF spaced receiver system (e.g.,

Bhattacharyya et al., 2003; Sharma, Chavan, et al., 2017; Sharma et al., 2018), Fabry-Pérot interferometer (e.g., Sahai et al., 1992), GPS (e.g., Haase et al., 2011; Ji et al., 2011; Nade et al., 2015), and ASI (e.g., Fagundes et al., 1997; Ghodpage et al., 2018; Kishore & Mukherjee, 2007; Nade et al., 2013; Pimenta, Bittencourt, et al., 2003; Sobral et al., 2009; Taori & Sindhya, 2014).

Sun et al. (2016) investigated the statistical features of EPBs using airglow images from 2012 to 2014, which lies in the increasing phase of 24th solar cycle from a ground-based network of four ASIs in the equatorial region of China. They calculated zonal drift for the period of March–April 2012 to 2014 and found that EPBs usually have a maximum drift near 100 m/s at 21:00–22:00 LT in  $9.5^\circ \pm 1.5^\circ$  geomagnetic latitude and then decrease to 50–70 m/s toward dawn period. Also, during March–April from 2012 to 2014, the peak velocities gradually increased from 70, 105, and 120 m/s, respectively. This indicates that the drift is solar activity dependent over Chinese longitudinal sector. They also suggest that the strong yearly variation of EPBs' drift velocities during March–April of 2012 to 2014 is very likely to be related to the background zonal neutral winds, which are the main driver for the background plasma drifts that produce eastward drifts. This means that the gradually increasing zonal drift velocities during March–April of 2012 to 2014 could suggest gradually increasing background zonal neutral winds during these years.

From the previous literature, it is well believed that the EPBs are initially generated at the bottomside of the  $F$  region through a fluid type gradient instability mechanism such as generalized Rayleigh-Taylor (R-T) instability (Abdu et al., 2009) in conjunction with  $E \times B$  instability. The requirements for this R-T instability growth are the post sunset rise of the  $F$  region, the availability of a seed perturbation to trigger the R-T mechanism, and the absence of a strong transequatorial thermospheric wind (Mendillo et al., 1992). Mukherjee and Shetti (2008) using photometer observations made over Kolhapur observed the dominant periodicities in OI 630.0-nm intensity fluctuations on a spread  $F$  night, which were typically varying between 30 and 50 min. Further, they suggested that this could be the typical wave periods of the gravity waves that produce the perturbation electric fields, which causes the growth of the plumes in ESF. Hysell et al. (1990) showed that the quasiperiodic *bubbles* or ESF could be *seeded* by gravity waves having horizontal wavelengths of the order of 100 km at altitudes of around 200 km (the bottom of the  $F$  layer). Huang et al. (1990), using simultaneous observations of ionospheric total electron content depletions associated with amplitude scintillations at three spaced locations on Taiwan Island, investigated the eastward zonal drift motions of the total electron content depletions during January 1986 to December 1988. They found that the most probable eastward drift ranges from 64 to 130 m/s with a mean drift of 97 m/s. Ghodpage et al. (2014) reported the zonal drift velocity of EPBs using 630.0-nm night airglow measurement carried out simultaneously from Kolhapur (16.8°N, 74.2°E, 10.6°N dip latitude) and Gadanki (13.5°N, 79.2°E, 6.5°N dip latitude) during March 2012. Their results show that the drift velocity for Kolhapur varies from 124 to 181.8 m/s, while for the Gadanki the drift velocity varies from 116.3 to 160.3 m/s. Fagundes et al. (1997) used an all-sky imaging system for observations of the 630.0-nm nightglow emission over Cachoeira Paulista (22.7°S, 45.0°W, 16°S dip latitude), Brazil, and calculated the vertical and zonal velocities of the plasma bubbles. They found that the zonal plasma drift exhibited some values ( $>300$  m/s) larger than those reported by Mendillo and Baumgardner (1982;  $\sim 200$  m/s). Sobral et al. (1999) studied the variation in the zonal drift of EPBs using zonal scanning photometer measurements of the nocturnal 630.0-nm airglow for the period of 1980–1992 over Cachoeira Paulista. The central motivation of their work is to investigate the effects of the solar activity and geomagnetic activity on the zonal drift of EPBs. They observed that the zonal drift decays faster between 21:00 and 02:00 LT during the period of maximum solar activity than during the solar minimum period. They also found that the quiet night zonal drift in March months tended to increase with respect to disturbed night zonal drift with local time whereas in October such tendency was the opposite. Terra et al. (2004) presented a statistical study of the zonal drift velocities of the plasma bubbles using scanning ( $\pm 75^\circ$  around zenith in the east-west direction) photometer airglow data acquired at the low-latitude station Cachoeira Paulista, during the period of October to March, between 1980 and 1994. Their results showed that the velocities are larger during the solar maximum activity period and tend to increase with  $F_{10.7}$  solar flux during the premidnight period. Also, it can be observed that these velocities tend to decrease faster with local time during solar minimum than during solar maximum.

In present study we used ASI data for 12 months, January to April as common months among 3 years, 2011 to 2013. The data for October, November, and December 2013 are not available so that the common months from all these three years are chosen. The effect of solar and magnetic activity on the zonal drift velocity

**Table 1**  
Summary of Observation Nights From January to April of Three Years (2011–2013)

Year	Months	Total number of observation nights (event nights)	Total number of images recorded	Event images	Occurrence (%)
2011	January	14 (02)	1,392	195	14.00
	February	13 (08)	1,320	362	27.42
	March	17 (06)	1,607	499	31.05
	April	13 (06)	1,295	427	32.97
	Total	57 (22)	5,614	1,483	Average: 26.36
2012	January	14 (08)	1,627	574	35.27
	February	15 (07)	1,477	432	29.24
	March	13 (07)	1,225	380	31.02
	April	11 (02)	1,127	116	10.29
	Total	53 (24)	5,456	1,502	Average: 26.45
2013	January	9 (02)	852	138	16.19
	February	10 (02)	895	68	7.59
	March	8 (03)	685	187	27.29
	April	11 (05)	957	419	43.78
	Total	38 (12)	3,389	812	Average: 23.71
Grand total		143 (58)	14,459	3,797	

of EPBs has been studied. Kolhapur is located in between the dip equator and the northern crest of the equatorial ionospheric anomaly (EIA), which is being a unique place to study the electrodynamical coupling in  $E$  and  $F$  regions using nightglow OI 630.0-nm emission data (Nade et al., 2013).

## 2. Instrumentation and Methodology

The ASI is installed in 2009 under scientific collaboration between Shivaji University, Kolhapur (S.U.K.), and Indian Institute of Geomagnetism (I.I.G.), Navi Mumbai, at Shivaji University Campus, Kolhapur (16.8°N, 74.°E; 10.6°N dip latitude). ASI observation is carried out 7 days before and after new moon night to study the night airglow emission. The quantum efficiency of the ASI is >95%. Low dark current (0.5 electrons per pixel per second) with low readout noise and high linearity of ASI is useful to achieve quantitative observations of the nightglow emissions. A high-resolution (1,024 × 1,024 pixels), charge-coupled device (CCD)-based ASI has 180° FOV with fisheye lens (f/4 Mamiya RB67) at top having focal length of 24 mm and telecentric lens system, which is used to collect light from the night sky. The CCD detector is back illuminated with an array of 1,024 × 1,024 pixels and 16-bit resolution. Before the operation, dark counts are reduced by thermoelectric cooling (−80 °C) of CCD. For the present study, ASI is operated in three filters OI 630.0 nm, OI 557.7 nm, and OH emission. But, in present case, we dealt only with the OI 630.0-nm emission to study the EPBs. The images recorded by ASI appear curved and compressed at lower elevation angles. This occurs because the

lens projects an image onto the CCD such that each pixel subtends an equal angle of the sky. To avoid this curvature effect, we have not considered the EPBs beyond 100° FOV into account. Also, the FOV is kept 140° for campaign observations to avoid city light noise and local interference. The detailed information of ASI has been introduced by Ghodpage et al. (2014). The images recorded by ASI are processed using the processing method described by Sharma et al. (2014).

## 3. Methodology

Pimenta et al. (2001) proposed scanning method to determine the zonal drift of EPBs. This method was also used by Nade et al. (2013) using ASI image data of OI 630.0-nm emission for the determination of zonal drift velocity over Kolhapur station. The zonal drift velocity of EPBs can be calculated by comparing its positions in consecutive images to find the longitudinal offset and dividing it by the time difference between the images (Makela et al., 2005). To determine the longitudinal offset or shifting of EPBs in terms of pixels, we have designed MATLAB code to analyze one night (~100 images) ASI data at a time. Figure 1c is the illustration of pixel measurements in 140° and 100° FOV for all-sky images. The outer yellow circle refers to 140° FOV, and inner red circle refers to 100° FOV. For the 100° FOV, in 1,024 × 1,024 ASI image, the diameter of the image is ~568 pixels (i.e., 794 pixel minus 226 pixel). The yellow strip drawn in Figure 1c along east-west direction is of the size of 20 pixels (±10 pixels to either side of zenithal line). The average intensity of each image along this strip is measured. These intensity data for each image in whole night can be exported to excel file. The intensity is then plotted against pixel numbers for each images as shown in Figure 1d. The signature of EPBs is seen in the scan curve as downward troughs moving toward east. The shifting of the center of EPBs is measured in terms of pixels. These pixels are converted into kilometers using the conversion values described in Sharma et al. (2014; See their Figure 4 and Table 1). Once the distance covered by EPB is known, with time difference between two successive images, the velocity can be determined easily.

## 4. Results and Discussion

### 4.1. Daily Hourly Zonal Drift Velocity Variation

Over 143 nights of observations are made using ASI with OI 630.0-nm emission during January to April of 2011 to 2013. The summary of data considered for present study is shown in Table 1. Out of which 58

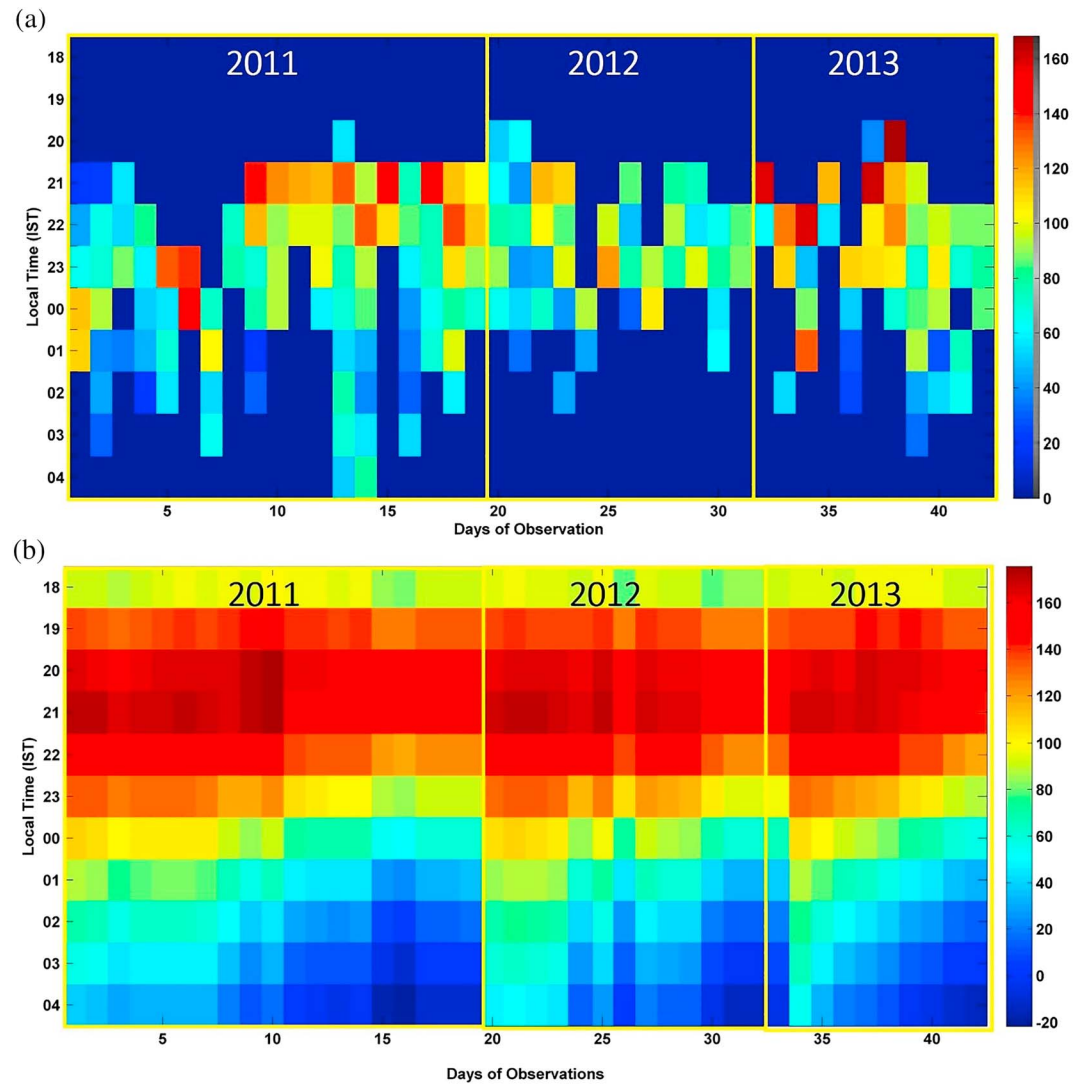


**Figure 2.** (a) Daily hourly variation in zonal drift velocity of equatorial plasma bubbles for the days of observations from 2011 to 2013. (b) HWM plot of daily hourly variation in zonal drift velocity of equatorial plasma bubbles for the days of observations from 2011 to 2013.

nights show signatures of EPBs. Further, 42 nights are eligible for zonal drift velocity measurement according to the method described in section 3. Here we take east-west scan with 20 pixel strip around zenith; there are certain nights on which EPBs do not reach at zenith so their zonal drift cannot be measured with this technique. The occurrence of scintillation (caused due to presence of EPBs) at any station situated off the magnetic equator depends on the height to which EPBs develops under  $E \times B$  (Kumar & Gwal, 2000). So in this case EPBs' height might be lesser (due to insufficient prereversal enhancement), which are unable to map to zenith latitude (i.e.,  $16.8^\circ\text{N}$ ) and are excluded from this study. The EPBs appeared in the image covering the full FOV are better for zonal drift measurement. The zonal drift velocity has been successfully measured for 42 nights and plotted against local time as shown in Figure 2a. It is a contour of three variables, time (IST) being at Y axis, days of observations being at X axis, and the drift velocity being at Z axis indicated by colored vertical bar at the extreme right. This plot is categorized according to years as shown by yellow rectangles, which distinguish it. It is found that the zonal drift velocity peak appears between 21:00 and 22:00 LT and decreases toward remaining course of night (LT = UT + 05:30 hh:mm). It has peaked up to  $\sim 145$  m/s in the year 2011 and  $\sim 165$  m/s in the year 2013. In the year 2012 it is  $\sim 125$  m/s, which is lower than 2011. This might be due to less density of data available in the year 2012.

But the important thing to be noted here is that the zonal drift velocity has increased from  $\sim 145$  to  $\sim 165$  m/s from 2011 to 2013, respectively. The year 2013 is being a near solar maximum year; this is why the zonal drift velocity of EPBs is found maximum in this year.

Generally, the initial EPBs' onset occurs in the early evening hours at 19:15–20:00 LT and is followed by eastward propagation with an average speed of 90–120 m/s prior to local midnight and rapidly decreasing around the midnight and postmidnight periods (Chapagain et al., 2012). Kishore and Mukherjee (2007) studied EPBs over Kolhapur and found that they are normally confined to the time interval between 21:00 and 01:00 LT. In our case the zonal drift velocity has peaks before almost midnight. To support this finding, we have checked the hourly variation in zonal drift velocity obtained from HWM-07 model for the period under consideration. The HWM-07 provides a statistical representation of the horizontal wind fields of the Earth's atmosphere from the ground to the exosphere (0–500 km). It estimates the atmospheric wind using satellite, rocket, and ground-based wind measurement's data of over 50 years (Drob et al., 2008). Also it is stated that the zonal drift velocity of EPBs and the zonal neutral wind velocity obtained from HWM-07 model show that the nighttime plasma moves along with the neutral zonal wind (Basu et al., 1996). Further, the *F* region neutral winds are the major source of the electric fields governing the plasma motion in the tropical latitudes. The HWM-07 model plot for the hourly zonal drift velocity is shown in Figure 2b. There is no notable variation observed in HWM-07 model plot as compared to Figure 2a. Therefore, we have checked the peak drift velocities on each nights both in observed measurements and the model measurements and compared this with the corresponding daily averaged 10.7-cm solar flux. Figures 3a and 3b show the peak drift velocity on each observation night versus daily averaged solar fluxes for observed peak drift velocity and the HWM-07 model peak drift velocity, respectively. It is clearly observed that the peak drift velocity obtained from observed values and the model values has positive correlation with the 10.7-cm solar flux. The error bars shown in Figure 3a are the standard error of the data points. The daily average peak zonal drift velocities are found to be 125.13, 115.95, and 136.69 m/s for the years 2011, 2012, and 2013, respectively. Nade et al. (2013) studied the zonal drift velocity of EPBs for the period of October 2010 to May 2011 from Kolhapur using OI 630.0-nm images and found that the zonal drift velocity of EPB varies with solar activity (*F*10.7 cm) for magnetically quiet conditions. Also, the eastward average zonal drift velocity of EPBs increases from the evening sector ( $112 \pm 10$  m/s) to reach maximum about  $165 \pm 30$  m/s around 21:00 LT and then decreases toward dawn period. Previous researchers reported that the premidnight zonal drift velocities have a positive correlation with solar activity (e.g., Pimenta et al., 2001; Yao & Makela, 2007). Taori and Sindhya (2014) presented the ASI observations of OI 630.0-nm emission from Gadanki, India, and calculated the zonal drift of EPBs. They also found the positive correlation between zonal drift and solar flux.

#### 4.2. The Hourly Monthly Averaged Zonal Drift Velocity Variation

The hourly zonal drift velocity has been calculated for each month of January to April of 2011 to 2013 and is averaged month wise and plotted against local time as shown in Figure 4. The top row is for the year 2011, the middle row is for 2012, and the bottom row is for 2013. The red curves indicate the HWM-07 model zonal drift velocity for corresponding months. The black curve indicates the measured zonal drift velocity of EPBs, and the vertical bars denotes their standard deviation errors. It is seen that the drift peaks between 21:00 and 23:00 IST, that is, before midnight for almost all the months. Few months (January 2011 and 2012 and February 2011) have peak zonal drift velocity around midnight hours. It is known that the polarized electric field in the *F* region drives the plasma in the nighttime, and hence, the EPBs move eastward. In the postsunset period, the intensity of this electric field is very strong and decreases toward the remaining course of night due to reduced neutral wind velocity (Terra et al., 2004). Owing to this, the peaks in the drift of EPBs are generally before midnight under quiet conditions. Many researchers calculated the zonal drift of EPBs over Indian sector and observed that the drift peaks before midnight (e.g., Narayanan et al., 2017; Taori & Sindhya, 2014). Sometimes, the second peak may observe in the drift pattern around early morning hours as can be seen for March 2011 in Figure 4. One of the causes behind this is due to the disturbance dynamo electric fields, which suppress (enhance) the generation of EPBs in the postsunset (postmidnight) sector (e.g., Sun et al., 2012). With enhanced generation of EPBs (freshly generated EPBs) in the postmidnight sector, they might exhibit a greater polarized electric field, which is responsible for the increase in drift from usual decreasing trend during dawn period. It is also found that in the month of March (which is an equinoctial month) of all 3 years the zonal drift velocity is maximum as compared to any other months. Nade et al. (2013) also observed maximum

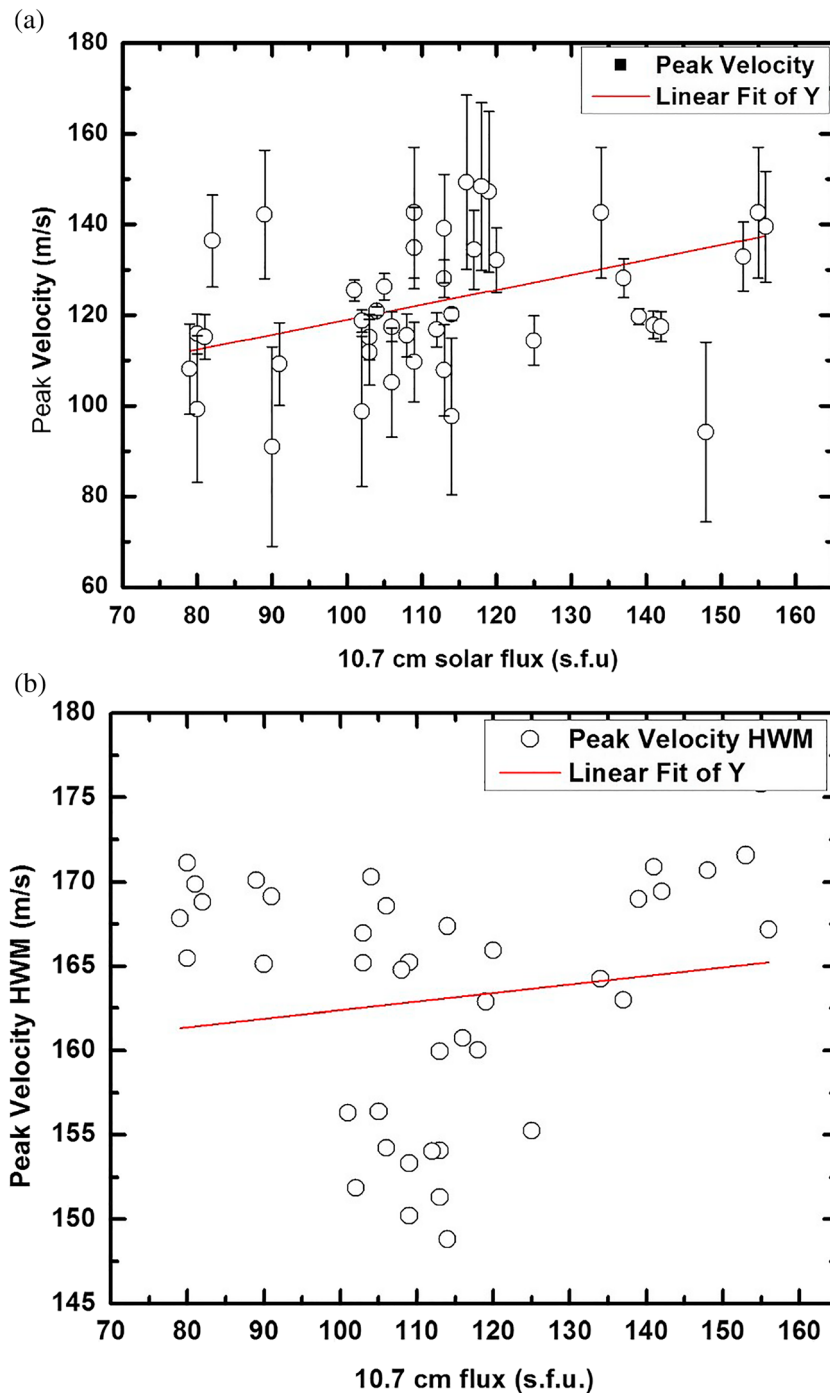


**Figure 3.** (a) Daily peak zonal drift velocity of equatorial plasma bubbles and the corresponding daily averaged 10.7-cm solar flux for all the observation days in 2011 to 2013. The red line is the linear fit, and the vertical bars depicts the standard error bars. (b) Daily peak zonal drift velocity of equatorial plasma bubbles obtained from HWM and the corresponding daily averaged 10.7-cm solar flux for all the observation days in 2011 to 2013. The red line is the linear fit.

zonal drift velocity in the month of March from the same location. The calculated zonal drift velocities presented herein are smaller than HWM-07 model values. Valladares et al. (2002) indicated that the relative velocities between winds and zonal drift velocity values vary depending on season and solar activity. The minor discrepancy if any in present case might due to the EPBs' growth phase and evolution over the course of night. One of the important things here is to note that, in March 2011, there is a prominent

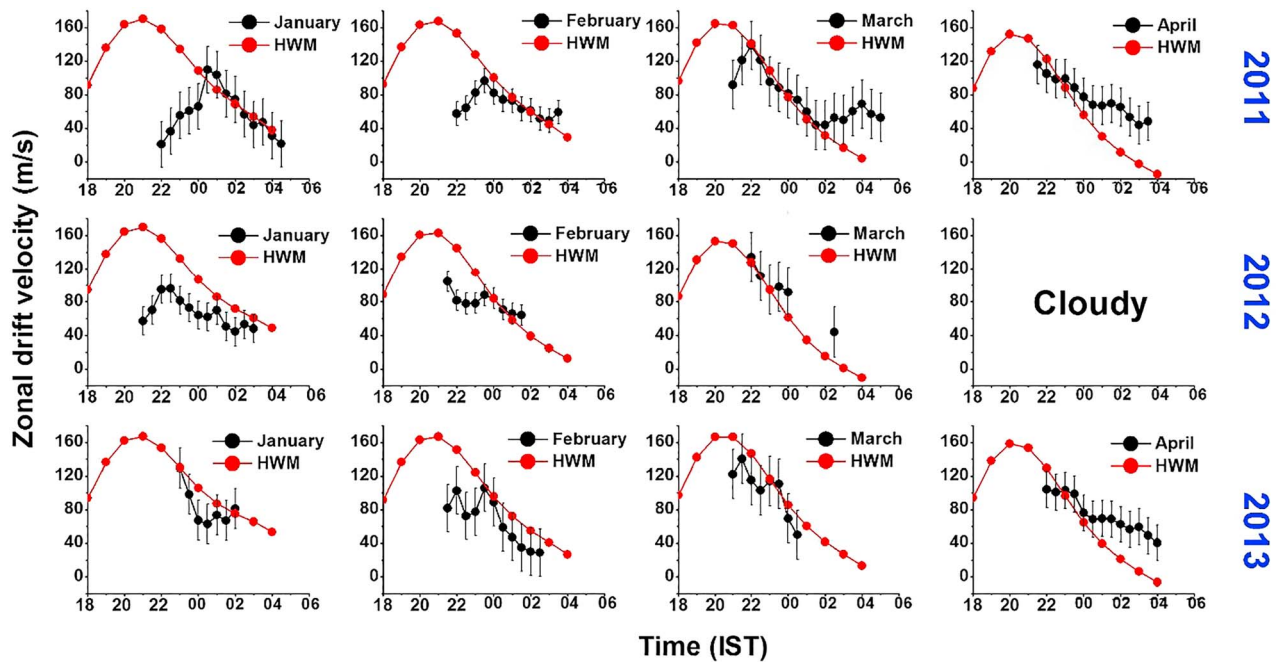


**Figure 4.** The hourly monthly averaged zonal drift velocity variation obtained from all-sky imager data and HWM data for the months of January to April of three years (2011–2013).

double peak in the zonal drift velocity one at 22:00 LT and another at 04:00 LT during dawn period. Sun et al. (2016) also observed a very prominent double-peak structure in the EPBs' zonal drift velocities toward dawn period during September–October 2013. We think that there could be a possibility of presence of second spaced  $F$  at equatorial region in the dawn hours, which might be responsible for this second peak seen in the zonal drift velocity at lower latitudes.

#### 4.3. The Hourly Seasonal Variation in Zonal Drift Velocity of EPBs

For seasonal analysis, we have considered March–April as equinoctial months and January–February as winter months (Vyas & Dayanandan, 2011). It is worthy to note that in summer months (May to August) the occurrence of EPBs is zero for Kolhapur location (Sharma, Gurav, et al., 2017). The zonal drifts for the March and April are averaged hourly to get the equinoctial variation. It is done similarly for the winter months. Figure 5 indicates the seasonal variation in the zonal drift velocity of EPBs for the years 2011–2013. The red and blue curves are the equinox and winter months, respectively. The black curves are the HWM-07 model plot of zonal drift velocity for corresponding months/season with respect to local time. It is found that the zonal drifts are larger remarkably in the equinox months than that of winter months. Moreover, the peaks in the zonal drifts occur at around 22:00 LT except in winter month of 2011. In Figure 5, the HWM-07 model values do not show notable difference in the zonal drift for equinox and winter months as can be seen in the observed values. Paulino et al. (2011), using airglow images observed at Sao Joao do Cariri (7.4°S, 36.5°W; dip angle:  $-11^\circ$ S), Brazil, from September 2000 to April 2007, calculated the plasma bubble zonal drifts for 97 geomagnetically quiet nights. They found that the EPBs observed during the summer months were moving faster than EPBs observed during the equinox months. But in our case the zonal drifts are larger in equinox months. So it encounters the discrepancy in the seasonal variation in the equinox months for both Indian and Brazilian sectors. This may be due to the longitudinal difference in the locations. Also, Pimenta, Fagundes, et al. (2003) used an all-sky imaging photometer, with OI 630.0-nm nightglow emission, from Cachoeira Paulista, Brazil, to determine the nocturnal monthly and latitudinal variation characteristics of the zonal plasma bubble drift velocities in the low latitude (16.7°S to 28.7°S) region. They observed that, after midnight, the eastward plasma bubble drift velocities decrease for both seasons (equinox and summer), but during equinox they reach lower velocities than in summer. In our case, HWM-07 model plots for equinox month's shows that the zonal drifts are tending to 0 and further becomes negative around 04:00 LT in the dawn period. However, the observed zonal drifts do not show such behavior



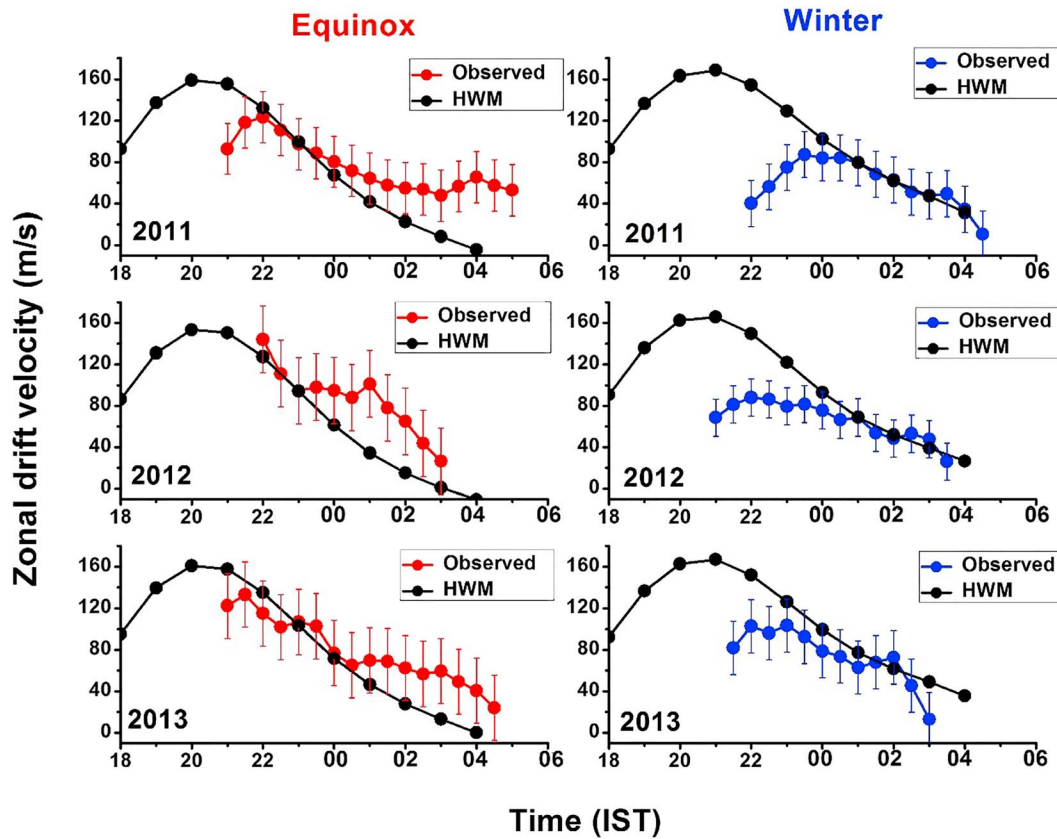


**Figure 5.** The seasonal variation in zonal drift velocity of equatorial plasma bubbles obtained from all-sky images and HWM data for the years 2011 to 2013.

**Table 2**  
Summary of Disturbed Night From 2011 to 2013 Used in the Study

Year	Day	% occurrence	$A_p$ index	10.7-cm flux	Remarks
2011	4 February	8	21	82	Less occurrence
	1 March	0	31	111	No occurrence
	10 March	10	20	131	Less occurrence
	11 March	0	40	123	No occurrence
	2 April	10	20	108	Less occurrence
	<b>6 April</b>	<b>48</b>	<b>26</b>	<b>117</b>	<b>Zenith</b>
	30 April	0	24	110	No occurrence
2012	22 January	20	21	141	Less occurrence
	<b>15 February</b>	<b>57</b>	<b>21</b>	<b>105</b>	<b>Zenith</b>
	15 March	24	30	111	Cloudy
	16 March	0	20	99	No occurrence
	23 April	0	23	142	No occurrence
	24 April	0	35	134	No occurrence
	25 April	0	21	127	No occurrence
2013	17 March	0	46	126	No occurrence

Note. Total number of disturbed nights: 14. The bold texts in the Table depict the nights having significant occurrence of equatorial plasma bubbles to study the drift variation.

but most importantly it is seen that the zonal drift after midnight is decreasing marginally faster for equinox months than that of winter months. Abdu et al. (1985) found that the bubble structures drift eastward at night and westward in the early morning, and the reversal of the zonal drift velocity occurs around 04:00 LT. This has been noted by HWM-07 values for the equinox months only in our case. Also, the EPBs are seen to vanish at this dawn period hours beyond 04:00 LT for Kolhapur location.

#### 4.4. The Zonal Drift Velocity Variation on Magnetically Disturbed Nights

Among all the 3-year data, we have separated the disturbed nights having  $A_p > 18$  (Chavan et al., 2016) as shown in Table 2. Sharma, Gurav, et al. (2017) studied the occurrence statistics of EPBs over Kolhapur for the period of 2011 to 2015 and found that the magnetic activity inhibits the occurrence. In present case, we have a total of 14 disturbed nights, out of which 8 nights do not show the occurrence of EPBs. In the remaining nights, four nights have less occurrence of EPBs and they are confined below  $16.8^\circ\text{N}$  and hence are not eligible to calculate the zonal drift velocity. We believe that, due to the influence of magnetic activity, there could be insufficient prereversal enhancement during the growth of EPBs, which caused EPBs to reach only at lower latitudes (smaller apex height). Only two nights, namely, 15–16 February 2012 and 6–7 April 2011, are having EPBs moving eastward over zenith and are considered for zonal drift measurements.

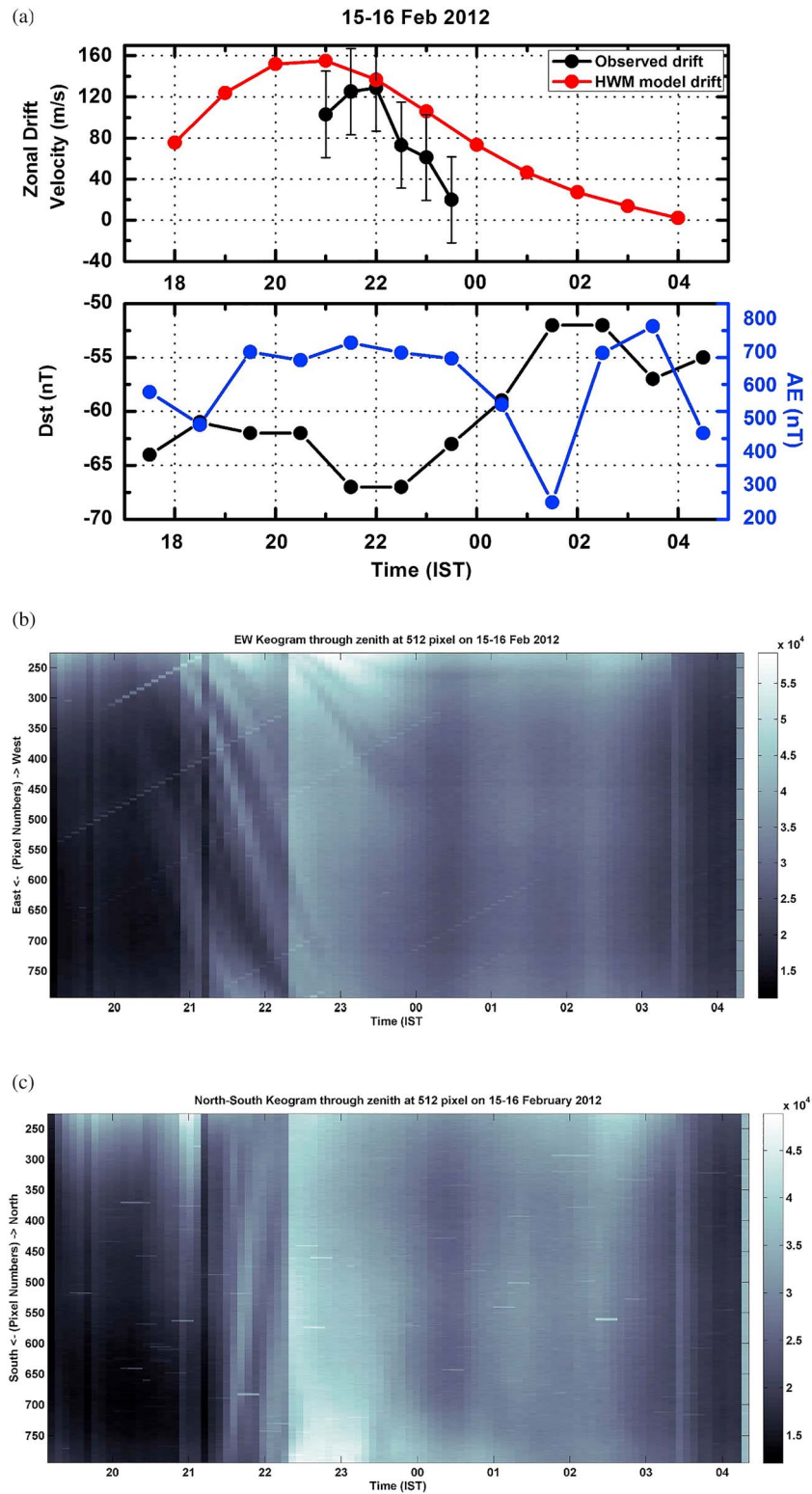
#### 4.4.1. Case I: 15–16 February 2012 ( $A_p = 21$ )

Figure 6a depicts the zonal drift measured using all-sky images (black curve) and HWM-07 model plot (red curve) in the top panels. The vertical bars in the black curve are the standard deviation error. The bottom panel indicates the hourly  $Dst$  indices (black curve) and the hourly  $AE$  indices (blue curve). The drift velocity peak ( $\sim 125$  m/s) occurred at 22:00 LT and then decreased toward dawn as low as 20 m/s. The  $Dst$  was minimum of  $-67$  nT around 22:00 LT, while  $AE$  indices shows moderate increment during this time. We have plotted the east-west and north-south keograms on this night to get the ensemble of whole night data. Figures 6b and 6c depict the east-west and north-south keograms, respectively. In Figure 6b, it can be seen that the EPBs have large velocity between 21:00 and 22:00 LT, and further, the drift seems to be suppressed between 22:00 and 00:00 LT. This can be understood by analyzing the slopes of the EPBs between 21:00 and 22:00 LT, which is larger and smaller between 22:00 and 00:00 LT. It is worthy here to note that after 22:00 LT the intensity of OI 630.0-nm emission (which is directly proportional to density of electrons in the ionosphere) increased up to midnight period in both the keograms. Further, the intensity enhancement is seen after midnight around 01:30 and 02:30 LT in both the keograms. Pimenta, Bittencourt, et al. (2003) observed that the increase in electron density within the equatorial ionospheric anomaly was sufficient to justify the observed reduction in the zonal wind velocities. In addition to this, they also suggested that this reduction in the ionospheric plasma bubble zonal drift velocities may be occurred due to a reduction in the zonal neutral wind. In the top panel of Figure 6a, it is seen that the drift velocity started increasing from 21:00 LT, peaked at 22:00 LT. It is then further started decreasing from 22:00 LT to midnight period where the intensity enhancement is observed in both the keograms. Also, after midnight the EPBs are disappeared from the all-sky images. This might be due to the accumulation of sufficient electron densities at ionospheric heights. We also suggest in agreement with Pimenta, Bittencourt, et al. (2003) that the reduction in zonal drift after 22:00 LT from 125 to almost 20 m/s might be due to the increase in electron density over EIA region, Kolhapur.

Sharma, Chavan, et al. (2017) studied the drifts of ionospheric irregularities (smaller scale) for the period January 2011 to December 2015 using amplitude scintillations data from VHF spaced receiver system installed at Kolhapur. They found that the zonal velocity pattern on magnetically disturbed nights shows reversal in the direction of usual eastward zonal drift around midnight. However, in our disturbed night, no westward drifts are seen and the EPBs drifts are found to be as low as 20 m/s around midnight and the EPBs are not seen during the remaining course of night. Sobral et al. (2009) analyzed in detail the zonal velocities of large-scale ionospheric plasma depletions over two conjugate stations (Boa Vista [22.0°N dip latitude] and Campo Grande [22.32°S dip latitude]) using OI 630-nm airglow all-sky images obtained during the Conjugate Point Equatorial Experiment campaign carried out in Brazil between October and November 2002. Their results show that the zonal velocity tends to decrease with increase in magnetic activity and tends to increase with increase in the solar flux. Martinis et al. (2003) presented studies of plasma drift using OI 630.0-nm measurements from South American sector. According to them (see their Table 1) the zonal plasma drifts, during night, were eastward during low magnetic activity while westward during moderate magnetic activity. Recently, Ghodpage et al. (2018) studied the ionospheric response to the major storm occurred on 17 March 2015 (being the strong geomagnetic activity with  $Dst$  as low as  $-222$  nT) using OI 630.0-nm all-sky images from Kolhapur. They found that, initially, EPBs were moving eastward ( $\sim 50$  m/s) and suddenly after 22:30 IST it started drifting westward and reached the negative value as  $-75$  m/s toward dawn. Pautet et al. (2009) studied the optical observations of the ionospheric OI (630 nm) emission layer conducted (as part of the SpreadFEx campaign) from two sites (Brasilia and Cariri) with similar magnetic latitudes and overlapping fields of view, in order to simultaneously study the plasma bubbles. They found the fossilized postmidnight EPBs on several nights, often until dawn, with lower eastward drift velocities (maximum  $\sim 50$  m/s). Occasionally, the drift velocity also showed a short-lived westward motion possibly due to a temporary reversal in the normal  $F$  layer dynamo electric field. From this scenario, it is concluded that the magnetic activity does effect on the drift of EPBs during the nighttime.

#### 4.4.2. Case II: 6–7 April 2011 ( $A_p = 26$ )

As explained in case I, we have plotted the zonal drift of EPBs (black curve) for this disturbed night and compared it with the HWM-07 model drift (top panel in Figure 7a). The vertical bars in the black curve is the standard deviation error. Also, the geomagnetic indices such as  $Dst$  (black curve) and  $AE$  (blue curve) are plotted as shown in bottom panel in Figure 7a. In this case the drift of EPBs peaked (125 m/s) at



**Figure 6.** (a) The top panel is the hourly variation in zonal drift velocity of equatorial plasma bubbles, and the bottom panel is the hourly averaged *Dst* and *AE* indices on disturbed nights of 15–16 February 2012. (b) East-west intensity keogram for the nights of 15–16 February 2012. (c) North-south intensity keogram for the nights of 15–16 February 2012.

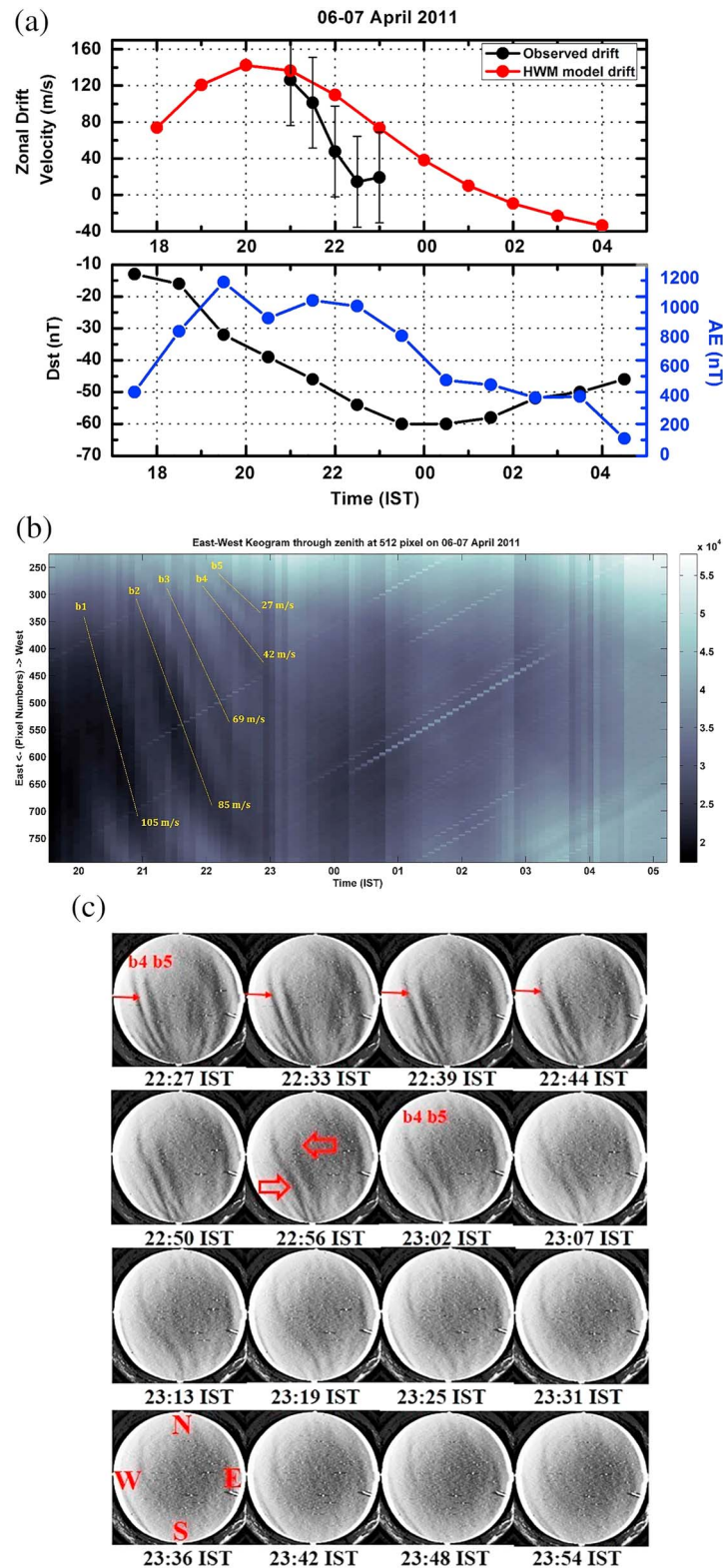


**Figure 7.** (a) The top panel is the hourly variation in zonal drift velocity of equatorial plasma bubbles, and the bottom panel is the hourly averaged *Dst* and *AE* indices on disturbed nights of 6–7 April 2011. (b) East-west intensity keogram through zenith at 512 pixel for the nights of 6–7 April 2011. (c) Sequences of processed images for the nights of 6–7 April 2011. (d) East-west keogram at 150 pixel toward north from zenith for the nights of 6–7 April 2011. (e) East-west at 150 pixel toward south from zenith for the nights of 6–7 April 2011.

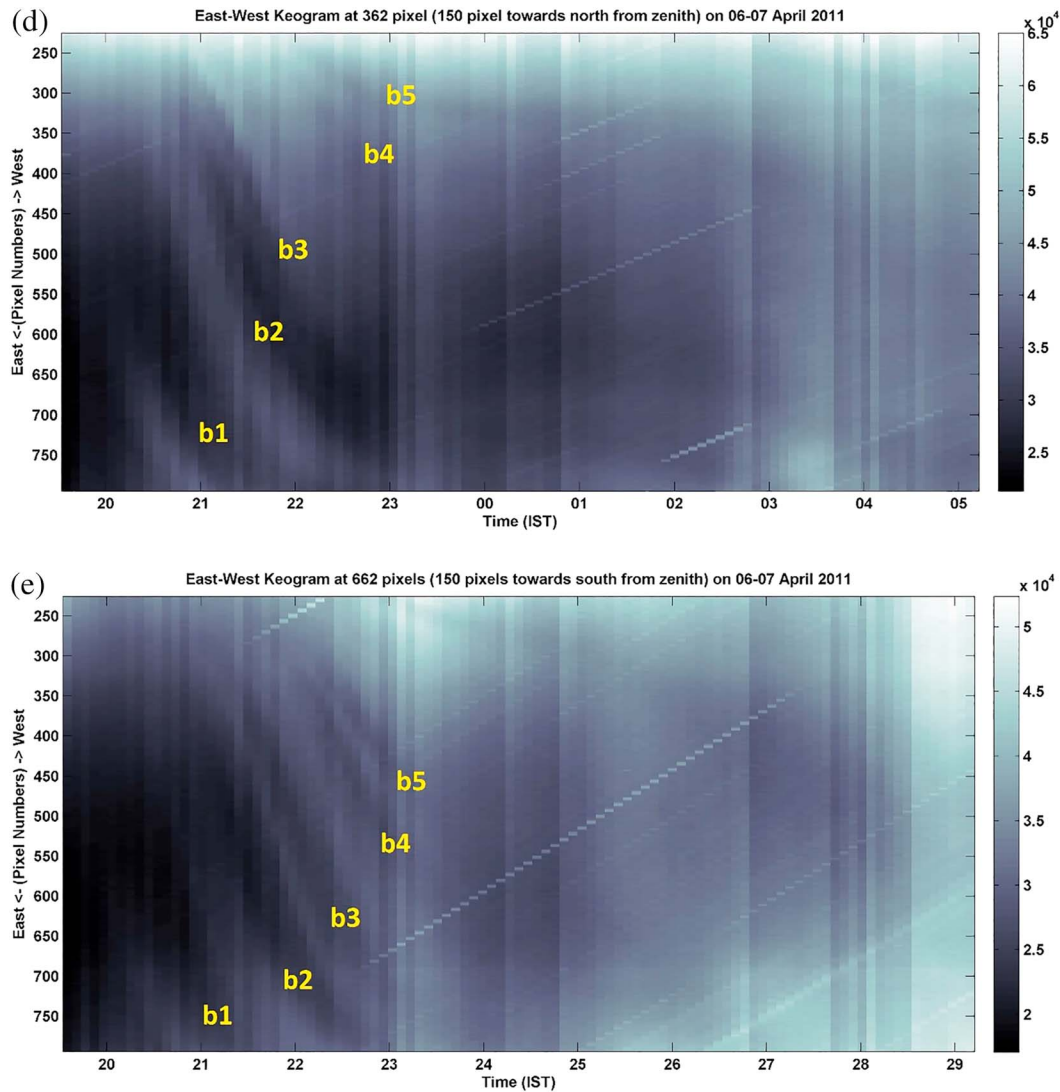


Figure 7. (continued)

21:00 LT and decreased toward dawn as low as 10 m/s. Also, EPBs are confined to the period of 21:00 to 23:00 LT. In this case, the *AE* index has intense fluctuations ( $\sim 1,100$  nT) as compared to case I; also, the *Dst* index was as low as  $-60$  nT. We have plotted the east-west keogram with 20 pixel strip around zenith for this night as shown in Figure 7b. There are five EPBs traversed in the FOV from west-east, namely b1, b2, b3, b4, and b5. It can be easily seen that the slopes (i.e., velocity) of these EPBs started decreasing from b1 to b5. The *AE* index that indicates the auroral electrojet activity sometimes becomes very intense and sustained during many hours, even in the absence of storms (Sobral et al., 2006). During the occurrence of such very intense *AE* activity, disturbance dynamo electric fields may be set up at low latitudes causing a reduction in the post sunset plasma eastward velocity (Abdu et al., 2003; Sobral et al., 2006). On this night, we observed the latitudinal variation in the zonal drifting of EPBs during the night. Figure 7c depicts the sequences of processed images on the nights of 6–7 April 2011. Initially, at 22:27 LT two EPBs are seen named as b4 and b5 moving eastward. As time progresses, the distance between these EPBs started increasing for couple of minutes and later on b5 tends to vanish toward midnight hours. In this journey, at 22:56 LT it is noted that the b4 and b5 have changed their shapes and became slant S shaped. The top portion of these two EPBs seems to be moving very slow (or rather seems to be stationary), while the bottom portion seems to be moving faster. This latitudinal

difference in their zonal motion caused the slant S shape. As time progresses, the b5 is seen to be almost vanished, while the b4 is still visible up to midnight hours.

Figures 7d and 7e depict the east-west keogram taken at  $\pm 150$  pixels toward north and south, respectively. It is seen in Figure 7d that the b4 and b5 are almost vanished and have smaller slopes (velocity). In Figure 7e, the b4 and b5 are still visible and have larger slopes (velocity). From this analysis it is observed that there could be a force from west to east which acted upon the northern part of FOV (see 22:56 IST image in Figure 7c) which reduced the zonal drift velocity of EPBs (b4 and b5), while the EPBs (b4 and b5) in southern part of FOV seems to be almost unaffected. Narayanan et al. (2017) carried out the all-sky imaging observations of OI 630.0 nm airglow from Panhala (16.8°N, 74.1°E; 11.1°N dip latitude), India, during January to March 2008. They found that the drifts of EPBs were lesser on disturbed nights than that of quiet nights. They suggested that this difference might occur due to the weakening of the *F* region dynamo caused by disturbed thermospheric winds. In addition to this, they observed the tilts of EPBs are larger on disturbed nights than the quiet nights. In present case, we suggest that the reduction in zonal drift or latitudinal variation in zonal drift occurred due to the disturbance dynamo electric field, which can be seen by the intense fluctuations in *AE* indices in Figure 7a.

Chapagain et al. (2012) studied OI (630.0 nm) airglow image data from Ascension Island (geographic: 7.9°S, 14.4°W; dip latitude: 16°S) in the southern Atlantic Ocean taken with the Utah State University all-sky CCD camera during 20 March to 7 April 1997 in order to study plasma bubbles occurring in the low-latitude nighttime ionosphere. One of their case studies (4–5 April 1997) demonstrates clear evidence of the shear velocity of a bubble structure. The magnitude of the shear velocity is up to 0.12 m/s with reversal from westward drift (20 m/s) at lower latitudes and eastward drift (up to 45 m/s) at higher latitudes. Subsequently, the bubble rotates counterclockwise and tilts eastward significantly. They stated that the westward reversal of the plasma bubble motion at lower latitudes (low apex altitudes) in a quiet geomagnetic condition probably results from a reversal in the *F* region dynamo or an increase in the altitude of the shear node in the nighttime *F* region plasma drift to altitudes above the peak altitude of the OI (630.0 nm) emission. The case studied by Chapagain et al. (2012) was a geomagnetically quiet night, however, we have studied the disturbed night zonal drift where we observed the latitudinal variation in zonal drift. Also, Pimenta, Bittencourt, et al. (2003) resolved that the ion drag from the equatorial ionospheric anomaly (EIA) causes the thermospheric neutral wind to have a latitudinal dependence in which velocities decrease with increasing latitudes.

## 5. Conclusions

The present study describes the variation in zonal drift velocity of EPBs during the increasing phase of 24th solar cycle using all-sky images with OI 630.0-nm emission from low latitude station Kolhapur. The main outcomes of the present study are summarized below:

- a) The zonal drift peaks around 22:00 LT and decreases toward dawn. The daily peak zonal drift velocity for the period of 2011 to 2013 is directly proportional to 10.7-cm solar flux; this indicates that the solar activity has strong influence on the zonal drift velocity of EPBs.
- b) The daily average peak zonal drift velocities are found to be 125.13, 115.95, and 136.69 m/s for the years 2011, 2012, and 2013, respectively. Here in the year 2012, the zonal drift velocity seems to be smaller due to comparatively low data availability than other years. But it can be concluded that the zonal drift velocity is larger in near solar maximum year (2013) than the near solar minimum year (2011).
- c) The zonal drift velocity is marginally larger in equinox months than that of winter months. Moreover, the zonal drift velocity decreases faster after midnight period for equinox months than that of winter months.
- d) The zonal drift velocity during disturbed conditions gets slower than usual drifts on quiet nights. Also, the velocity tends to minimum toward dawn on disturbed night.
- e) We observed the intense enhancement in OI 630.0-nm emission from 22:30 LT to midnight period where the EPBs' velocity is found to be reduced. Based on this observation, we suggest that the increased electron density in the ionospheric *F* region heights might have slowed down the zonal drift velocity of EPBs over Kolhapur.
- f) On the nights of 6–7 April 2011, the EPBs' shapes have been modified before midnight period and during this period EPBs have different drifts along the meridian. This latitudinal variation in zonal drift velocity

modified the shapes of EPBs during this period. At the north side of FOV the EPBs were moving with smaller velocity or rather stationary, while at the southern side of FOV EPBs have larger velocity. On this night AE index shows intense fluctuations, which may be the indication of electric field generated due to disturbance dynamo, which could be the reason behind the reduction in zonal drift velocity at the southern FOV of this location.

- g) The zonal drift velocities calculated and presented in this study are in good agreement with the previously reported literature. Further, our calculated values are a bit smaller than HWM-07 model values.

#### Acknowledgments

The ASI is installed by Indian Institute of Geomagnetism (I.I.G.), Navi Mumbai, India, at the campus of Shivaji University, Kolhapur (S.U.K.), under the scientific collaboration program. The night-airglow observations are made under this program. The data used in the present study can be accessed from Indian Institute of Geomagnetism (IIG) through S. Gurubaran (gurubara@iigs.iigm.res.in). O. B. Gurav is thankful to UGC-BSR, New Delhi, India, for financial support (F.25-1/2014-15(BSR)/7-167/2009/BSR, October 2015). We are thankful to the NOAA-GOES for providing the data of solar and geomagnetic indices over the Internet (ftp.swpc.noaa.gov/pub/warehouse). We also thank the SPDF, NASA, for providing the disturbance storm index (DST) data, which are available over the Internet ([https://omniweb.gsfc.nasa.gov/form/omni\\_min.html](https://omniweb.gsfc.nasa.gov/form/omni_min.html)).

#### References

- Abalde, J. R., Fagundes, P. R., Sahai, Y., Pillat, V. G., Pimenta, A. A., & Bittencourt, J. A. (2004). Height-resolved ionospheric drifts at low latitudes from simultaneous OI 777.4 nm and OI 630.0 nm imaging observations. *Journal of Geophysical Research*, *109*, A11308. <http://doi.org/10.1029/2004JA010560>
- Abdu, M. A., Batista, I. S., Reinisch, B. W., de Souza, J. R., Sobral, J. H. A., Pedersen, T. R., et al. (2009). Conjugate Point Equatorial Experiment (COPEX) campaign in Brazil: Electrodynamics highlights on spread F development conditions and day-to-day variability. *Journal of Geophysical Research*, *114*, A04308. <https://doi.org/10.1029/2008JA013749>
- Abdu, M. A., Batista, I. S., Sobral, J. H. A., de Paula, E. R., & Kantor, I. J. (1985). Equatorial ionospheric plasma bubble irregularity occurrence and zonal velocities under quiet and disturbed conditions from polarimeter observations. *Journal of Geophysical Research*, *90*(A10), 9921–9928. <https://doi.org/10.1029/JA090iA10p09921>
- Abdu, M. A., Batista, I. S., Takahashi, H., MacDougall, J., Sobral, J. H., Medeiros, A. F., & Trivedi, N. B. (2003). Magnetospheric disturbance induced equatorial plasma bubble development and dynamics: A case study in Brazilian sector. *Journal of Geophysical Research*, *108*(A12), 1449. <http://doi.org/10.1029/2002JA009721>
- Aggson, T. L., Laakso, H., Maynard, N. C., & Pfaff, R. F. (1996). In situ observations of bifurcation of equatorial ionospheric plasma depletions. *Journal of Geophysical Research*, *101*(A3), 5125–5132. <https://doi.org/10.1029/95JA03837>
- Basu, S., Kudeki, E., Basu, S., Valladares, C. E., Weber, E. J., Zengingonul, H. P., et al. (1996). *Journal of Geophysical Research*, *101*(A12), 26,795–26,809. <https://doi.org/10.1029/96JA00760>
- Bhattacharyya, A., Groves, K. M., Basu, S., Kuenzler, H., Valladares, C. E., & Sheehan, R. (2003). L-band scintillation activity and space-time structure of low-latitude UHF scintillations. *Radio Science*, *38*(1), 1004. <http://doi.org/10.1029/2002RS002711>
- Candido, C. M. N., Batista, I. S., Becker-Guedes, F., Abdu, M. A., Sobral, J. H. A., & Takahashi, H. (2011). Spread F occurrence over a southern anomaly crest location in Brazil during June solstice of solar minimum activity. *Journal of Geophysical Research*, *116*, A06316. <http://doi.org/10.1029/2010JA016374>
- Chapagain, N. P., Taylor, M. J., Makela, J. J., & Duly, T. M. (2012). Equatorial plasma bubble zonal velocity using 630.0 nm airglow observations and plasma drift modeling over Ascension Island. *Journal of Geophysical Research*, *117*, A06316. <http://doi.org/10.1029/2012JA017750>
- Chavan, G. A., Sharma, A. K., Gurav, O. B., Gaikwad, H. P., Nade, D. P., Nikte, S. S., et al. (2016). Dependence of Coherence Scales of Ionospheric Scintillation Patterns on Magnetic Activity. MAPAN-Journal of Metrology Society of India. <https://doi.org/10.1007/s12647-016-0191-3>
- Drob, D. P., Emmert, J. T., Crowley, G., Picone, J. M., Shepherd, G. G., Skinner, W., et al. (2008). An empirical model of the Earth's horizontal wind fields: HWM07. *Journal of Geophysical Research*, *113*, A12304. <https://doi.org/10.1029/2008JA013668>
- Fagundes, P. R., Sahai, Y., Batista, I. S., Bittencourt, J. A., Abdu, M. A., & Takashi, H. (1997). Vertical and zonal equatorial F-region plasma bubble velocities determined from OI 630 nm nightglow imaging. *Advances in Space Research*, *20*(6), 1297–1300. [http://doi.org/10.1016/S0273-1177\(97\)00790-4](http://doi.org/10.1016/S0273-1177(97)00790-4)
- Fejer, B. G., dePaula, E. R., Gonzales, S. A., & Woodman, R. F. (1991). Average vertical and zonal F region plasma drifts over Jicamarca. *Journal of Geophysical Research*, *96*(A8), 13,901–13,906. <https://doi.org/10.1029/91JA01171>
- Ghodpage, R. N., Patil, P. T., Gurav, O. B., Gurubaran, S., & Sharma, A. K. (2018). Ionospheric response to major storm of 17th March 2015 using multi-instrument data over low latitude station Kolhapur (16.8°N, 74.2°E, 10.6° dip. Lat.). *Advances in Space Research*, *62*(3), 624–637. <http://doi.org/10.1016/j.asr.2018.05.003>
- Ghodpage, R. N., Taori, A., Patil, P. T., Gurubaran, S., Sripathi, S., Banola, S., & Sharma, A. K. (2014). Simultaneous optical measurements of equatorial plasma bubble (EPB) from Kolhapur (16.8°N, 74.2°E) and Gadanki (13.5°N, 79.2°E). *Journal of Atmospheric and Solar-Terrestrial Physics*, *121*, 196–205. <http://doi.org/10.1016/j.jastp.2014.05.008>
- Haase, J. S., Dautermann, T., Taylor, M. J., Chapagain, N., Calais, E., & Pautet, D. (2011). Propagation of plasma bubbles observed in Brazil from GPS and airglow data. *Advances in Space Research*, *47*(10), 1758–1776. <http://doi.org/10.1016/j.asr.2010.09.025>
- Huang, Y.-N. (1990). Drift motion of ionospheric bubbles at the equatorial anomaly crest region. *Journal of Geophysical Research*, *95*, 4297–4301. <https://doi.org/10.1029/JA095iA04p04297>
- Huba, J. D., Wu, T. W., & Makela, J. J. (2015). Electrostatic reconnection in the ionosphere. *Geophysical Research Letters*, *42*, 1626–1631. <http://doi.org/10.1002/2015GL063187>
- Hysell, D. L., Kelley, M. C., Swartz, W. E., & Woodman, R. F. (1990). Seeding and layering of equatorial spread F by gravity waves. *Journal of Geophysical Research*, *95*(A10), 17253. <http://doi.org/10.1029/JA095iA10p17253>
- Immel, T. J., Frey, H. U., Mende, S. B., & Sagawa, E. (2004). Global observations of the zonal drift speed of equatorial ionospheric plasma bubbles. *Annales Geophysicae*, *22*(9), 3099–3107. <https://doi.org/10.5194/angeo-22-3099-2004>
- Ji, S., Chen, W., Ding, X., & Zhao, C. (2011). Equatorial ionospheric zonal drift by monitoring local GPS reference networks. *Journal of Geophysical Research*, *116*, A08310. <http://doi.org/10.1029/2010JA015993>
- Kishore, M. H., & Mukherjee, G. K. (2007). Equatorial F region plasma drifts: A study using 630 nm emission of all sky images. *Current Science*, *93*(4).
- Kumar, S., & Gwal, A. K. (2000). VHF ionospheric scintillations near the equatorial anomaly crest: Solar and magnetic activity effects. *Journal of Atmospheric and Solar-Terrestrial Physics*, *62*(3), 157–167. [http://doi.org/10.1016/S1364-6826\(99\)00090-5](http://doi.org/10.1016/S1364-6826(99)00090-5)
- Makela, J. J., Kelley, M. C., & Su, S. Y. (2005). Simultaneous observations of convective ionospheric storms: ROCSAT-1 and ground-based imagers. *Space Weather*, *3*, S12C02. <https://doi.org/10.1029/2005SW000164>
- Makela, J. J., Ledvina, B. M., Kelley, M. C., & Kintner, P. M. (2004). Analysis of the seasonal variations of equatorial plasma bubble occurrence observed from Haleakala, Hawaii. *Annales Geophysicae*, *22*(9), 3109–3121. <https://doi.org/10.5194/angeo-22-3109-2004>

- Martinis, C., Eccles, J. V., Baumgardner, J., Manzano, J., & Mendillo, M. (2003). Latitude dependence of zonal plasma drifts obtained from dual-site airglow observations. *Journal of Geophysical Research*, 108(A3), 1129. <https://doi.org/10.1029/2002JA009462>
- Mendillo, M., & Baumgardner, J. (1982). Airglow characteristics of equatorial plasma depletions. *Journal of Geophysical Research*, 87(A9), 7641. <https://doi.org/10.1029/JA087iA09p07641>
- Mendillo, M., Baumgardner, J., Pi, X., & Sultan, P. J. (1992). Onset conditions for equatorial spread F. *Journal of Geophysical Research*, 97(A9), 13,865–13,876. <https://doi.org/10.1029/92JA00647>
- Mukherjee, G. K. (2003). Studies of equatorial F-region depletions and dynamics using multiple wavelength nightglow imaging. *Journal of Atmospheric and Solar-Terrestrial Physics*, 65(3), 379–390. [http://doi.org/10.1016/S1364-6826\(02\)00214-6](http://doi.org/10.1016/S1364-6826(02)00214-6)
- Mukherjee, G. K., & Shetti, D. J. (2008). Plasma drift motion in the F-region of the ionosphere using photometric nightglow measurements. *Indian Journal of Radio & Space Physics*, 37(4), 249–257.
- Nade, D. P., Sharma, A. K., Nikte, S. S., Patil, P. T., Ghodpage, R. N., Rokade, M. V., et al. (2013). Zonal velocity of the equatorial plasma bubbles over Kolhapur, India. *Annales Geophysicae*, 31(11), 2077–2084. <https://doi.org/10.5194/angeo-31-2077-2013>
- Nade, D. P., Shetti, D. J., Sharma, A. K., Taori, A., Chavan, G. A., Patil, P. T., et al. (2015). Geographical analysis of equatorial plasma bubbles by GPS and nightglow measurements. *Advances in Space Research*, 56(9), 1901–1910. <http://doi.org/10.1016/j.asr.2015.03.030>
- Narayanan, V. L., Gurubaran, S., Shiny, M. B. B., Emperumal, K., & Patil, P. T. (2017). Some new insights of the characteristics of equatorial plasma bubbles obtained from Indian region. *Journal of Atmospheric and Solar-Terrestrial Physics*, 156(August 2016), 80–86. <https://doi.org/10.1016/j.jastp.2017.03.006>
- Narayanan, V. L., Gurubaran, S., & Shiokawa, K. (2016). Direct observational evidence for the merging of equatorial plasma bubbles. *Journal of Geophysical Research: Space Physics*, 121, 7923–7931. <https://doi.org/10.1002/2016JA022861>
- Paulino, I., de Medeiros, A. F., Buriti, R. A., Takahashi, H., Sobral, J. H. A., & Gobbi, D. (2011). Plasma bubble zonal drift characteristics observed by airglow images over Brazilian tropical region. *Revista Brasileira de Geofísica*, 29(2), 239–246. <https://doi.org/10.1590/S0102-261X2011000200003>
- Pautet, P. D., Taylor, M. J., Chapagain, N. P., Takahashi, H., Medeiros, A. f., São Sabbas, F. T., & Fritts, D. C. (2009). Simultaneous observations of equatorial F-region plasma depletions over Brazil during the Spread-F Experiment (SpreadFEx). *Annales Geophysicae*, 27(6), 2371–2381. <https://doi.org/10.5194/angeo-27-2371-2009>
- Pimenta, A. A., Bittencourt, J. A., Fagundes, P. R., Sahai, Y., Buriti, R. A., Takahashi, H., & Taylor, M. J. (2003). Ionospheric plasma bubble zonal drifts over the tropical region: A study using OI 630 nm emission all-sky images. *Journal of Atmospheric and Solar-Terrestrial Physics*, 65(10), 1117–1126. [http://doi.org/10.1016/S1364-6826\(03\)00149-4](http://doi.org/10.1016/S1364-6826(03)00149-4)
- Pimenta, A. A., Fagundes, P. R., Bittencourt, J. A., Sahai, Y., Gobbi, D., Medeiros, A. F., et al. (2001). Ionospheric plasma bubble zonal drift: A methodology using OI 630 nm all-sky imaging systems. *Advances in Space Research*, 27(6–7), 1219–1224. [http://doi.org/10.1016/S0273-1177\(01\)00201-0](http://doi.org/10.1016/S0273-1177(01)00201-0)
- Pimenta, A. A., Fagundes, P. R., Sahai, Y., Bittencourt, J. A., & Abalde, J. R. (2003). Equatorial F-region plasma depletion drifts: Latitudinal and seasonal variations. *Annales Geophysicae*, 21(12), 2315–2322. <http://doi.org/10.5194/angeo-21-2315-2003>
- Sahai, Y., Aarons, J., Mendillo, M., Baumgardner, J., Bittencourt, J. A., & Takahashi, H. (1994). OI 630 nm imaging observations of equatorial plasma depletions at 16°S dip latitude. *Journal of Atmospheric and Terrestrial Physics*, 56(11), 1461–1475. [http://doi.org/10.1016/0021-9169\(94\)90113-9](http://doi.org/10.1016/0021-9169(94)90113-9)
- Sahai, Y., Takahashi, H., Fagundes, P. R., Clemesha, B. R., Teixeira, N. R., & Bittencourt, J. A. (1992). Observations of thermospheric neutral winds at 23°S. *Planetary and Space Science*, 40(6), 767–773. [http://doi.org/10.1016/0032-0633\(92\)90105-W](http://doi.org/10.1016/0032-0633(92)90105-W)
- Sharma, A. K., Chavan, G. A., Gurav, O. B., Gaikwad, H. P., Ghodpage, R. N., & Nade, D. P. (2017). Dynamics of ionospheric irregularities in increasing phase of 24th solar cycle at Kolhapur [16.4°N, 74.2°E]. *Advances in Space Research*, 60(10), 2195–2205. <http://doi.org/10.1016/j.asr.2017.08.002>
- Sharma, A. K., Gurav, O. B., Chavan, G. A., Gaikwad, H. P., Ghodpage, R. N., & Patil, P. T. (2017). Variation in occurrence of equatorial plasma bubbles (EPBs) using all sky imager from low latitude station Kolhapur (16.8°N, 74.2°E, 10.6° dip. Lat.). *Advances in Space Research*, 60(11), 2452–2463. <http://doi.org/10.1016/j.asr.2017.09.014>
- Sharma, A. K., Gurav, O. B., Gaikwad, H. P., Chavan, G. A., Nade, D. P., Nikte, S. S., et al. (2018). Study of equatorial plasma bubbles using all sky imager and scintillation technique from Kolhapur station: A case study. *Astrophysics and Space Science*, 363(4). <http://doi.org/10.1007/s10509-018-3303-4>
- Sharma, A. K., Nade, D. P., Nikte, S. S., Ghodpage, R. N., Patil, P. T., Rokade, M. V., et al. (2014). Development of fast image analysis technique for all-sky images. *Current Science*, 1–9.
- Sinha, H. S. S., & Raizada, S. (2000). Some new features of ionospheric plasma depletions over the Indian zone using all sky optical imaging. *Earth, Planets and Space*, 52(8), 549–559. <https://doi.org/10.1186/BF03351662>
- Sobral, J. H. A., Abdu, M. A., Gonzalez, W. D., Gonzalez, A. C., Tsurutani, B. T., Da Silva, R. R. L., & Guarnieri, F. (2006). Equatorial ionospheric responses to high-intensity long-duration auroral electrojet activity (HILDCAA). *Journal of Geophysical Research*, 111, A07502. <http://doi.org/10.1029/2005JA011393>
- Sobral, J. H. A., Abdu, M. A., Pedersen, T. R., Castilho, V. M., Arruda, D. C. S., Muella, M. T. A. H., et al. (2009). Ionospheric zonal velocities at conjugate points over Brazil during the COPEX campaign: Experimental observations and theoretical validations. *Journal of Geophysical Research*, 114, A04309. <http://doi.org/10.1029/2008JA013896>
- Sobral, J. H. A., Abdu, M. A., Takahashi, H., Sawant, H., Zamlutti, C. J., & Borba, G. L. (1999). Solar and geomagnetic activity effects on nocturnal zonal velocities of ionospheric plasma depletions. *Advances in Space Research*, 24(11), 1507–1510. [http://doi.org/10.1016/S0273-1177\(99\)00716-4](http://doi.org/10.1016/S0273-1177(99)00716-4)
- Sun, L., Xu, J., Wang, W., Yuan, W., Li, Q., & Jiang, C. (2016). A statistical analysis of equatorial plasma bubble structures based on an all-sky airglow imager network in China. *Journal of Geophysical Research: Space Physics*, 121, 11,495–11,517. <http://doi.org/10.1002/2016JA022950>
- Sun, Y. Y., Liu, J. Y., & Lin, C. H. (2012). A statistical study of low latitude F region irregularities at Brazilian longitudinal sector response to geomagnetic storms during post-sunset hours in solar cycle 23. *Journal of Geophysical Research*, 117, A03333. <https://doi.org/10.1029/2011JA017419>
- Taori, A., Jayaraman, A., & Kamalakar, V. (2013). Imaging of mesosphere-thermosphere airglow emissions over Gadanki (13.5°N, 79.2°E)—First results. *Journal of Atmospheric and Solar-Terrestrial Physics*, 93, 21–28. <http://doi.org/10.1016/j.jastp.2012.11.007>
- Taori, A., & Sindhya, A. (2014). Measurements of equatorial plasma depletion velocity using 630 nm airglow imaging over a low-latitude Indian station. *Journal of Geophysical Research: Space Physics*, 119, 1–6. <http://doi.org/10.1002/2013JA019465>
- Terra, P. M., Sobral, J. H. A., Abdu, M. A., Souza, J. R., & Takahashi, H. (2004). Plasma bubble zonal velocity variations with solar activity in the Brazilian region. *Annales Geophysicae*, 22(9), 3123–3128. <http://doi.org/10.5194/angeo-22-3123-2004>



- Valladares, C. E., Meriwether, J. W., Sheehan, R., & Biondi, M. A. (2002). Correlative study of neutral winds and scintillation drifts measured near the magnetic equator. *Journal of Geophysical Research*, *107*(A7), 1112. <http://doi.org/10.1029/2001JA000042>
- Vyas, B. M., & Dayanandan, B. (2011). Nighttime VHF ionospheric scintillation characteristics near the crest of Appleton anomaly station, Udaipur (24.6°N, 73.7°E). *Indian Journal of Radio & Space Physics*, *40*(4), 191–202.
- Wu, K., Xu, J., Wang, W., Sun, L., Liu, X., & Yuan, W. (2017). Interesting equatorial plasma bubbles observed by all-sky imagers in the equatorial region of China. *Journal of Geophysical Research: Space Physics*, *122*, 10,596–10,611. <http://doi.org/10.1002/2017JA024561>
- Yao, D., & Makela, J. J. (2007). Analysis of equatorial plasma bubble zonal drift velocities in the Pacific sector by imaging techniques. *Annales Geophysicae*, *25*(3), 701–709. <https://doi.org/10.5194/angeo-25-701-2007>